

Performance of Separation Models to Predict Direct Irradiance at High Frequency: Validation over Arid Areas

Christian A. Gueymard¹ and Jose A. Ruiz-Arias²

¹ Solar Consulting Services, Colebrook, NH, USA

² Department of Applied Physics I, University of Málaga, Málaga, Spain

Abstract

A comprehensive study of the performance of 36 separation models selected from the literature is presented here, using high-quality 1-min data of global horizontal irradiance (GHI) and direct normal irradiance (DNI), toward the evaluation of the uncertainty in GHI-derived DNI. A detailed performance assessment is conducted from 9 stations over arid or desert areas of 5 continents, where the solar resource is high and solar systems have great potential. To evaluate the performance of each model, three summary statistics are calculated. The random errors are found significant, even though the test stations have only low cloudiness compared to temperate climates. For some models, the errors are exacerbated by cloud enhancement effects. The uncertainty in the predicted DNI appears highly dependent on the local radiation climate, the specific separation model, and the number of predictors used. The two Perez models, which both use a variability predictor, are most generally those generating the best predictions, although they conversely have more bias than simpler models, and may occasionally generate spurious results.

Keywords: Direct-diffuse separation; DNI; irradiance variability; cloud enhancement; validation.

1. Introduction

The successful development of solar power requires precise solar resource information, particularly in terms of direct normal irradiance (DNI). This is essential for concentrating solar power (CSP) or concentrating PV (CPV) systems, most particularly. Such systems are increasingly being deployed over arid areas, where cloudiness is low and solar resource is high. One difficulty is that, in most cases, DNI must be derived from measured or modeled global horizontal irradiance (GHI), by performing its “separation” or “decomposition” into the direct and diffuse (DIF) components. This is done systematically, for instance, to produce time series of DNI when GHI is derived from satellite imagery with the common “cloud index” method.

Separation models are empirical by design, consist of locally- or regionally-adjusted functions, and are derived from data measured most usually at temperate sites. Their accuracy is therefore not verified yet over arid or desert areas, where many conditions are different: Cloud regime, aerosol loading, and ground albedo, most importantly. The separation process is a major source of uncertainty when used in the derivation of the global tilted irradiance used by PV plants (Gueymard, 2009). Furthermore, the proper simulation of CSP projects requires solar radiation data at time steps shorter than the customary hourly interval. This is because of the non-linear and transient effects that substantially affect those systems, for which an ideal simulation time step would be of the order of 10 minutes or less (Hirsch et al., 2010).

In parallel, modern radiometric stations typically report irradiance data as 1- to 10-min averages, while some commercial providers of satellite-derived irradiance data time series can now provide data at 10- to 15-min time steps, in addition to the more usual hourly frequency. However, in satellite-derived data, the production of DNI and DIF still relies on empirical separation models developed from and for hourly irradiances, again usually obtained using data from temperate sites. A validation of these methods over arid environments and at sub-hourly time steps is thus desirable, which is the focus of this contribution. To this end, 1-min data

from 9 sites in diverse environments over five continents and at various elevations are used. The objectives of this study are multiple: (i) Validate existing separation models at the 1-min data time step; (ii) Determine which model(s) could potentially be of universal validity under arid conditions; (iii) Determine whether adding predictors can effectively improve the performance of models; and (iv) Evaluate model performance under high irradiance conditions.

2. Separation models

The literature has been searched for separation models using GHI at hourly or sub-hourly time steps. In most cases, the diffuse fraction, K , (i.e., the DIF/GHI ratio), from which DNI can be easily derived via the radiation closure equation, is first evaluated from the clearness index, K_t , (the ratio of GHI to its extraterrestrial counterpart). A few other models rather derive DNI more directly from K_t , through a functional relationship between it and the direct transmittance of the atmosphere, K_n , which in turn provides DNI. (Note that the fundamental closure relationship $K_n = K_t(1-K)$ is convenient to easily intercompare all these models.) Following a thorough literature search, 90 separation models have been found in scientific journals, conference proceedings or reports, which is an indication of the importance of this topic, and of its vitality since the 1960s. Due to space limitations, only 36 of these models are benchmarked here. The models under scrutiny have been selected as follows: (i) those most frequently cited in the literature and/or being used operationally to derive DNI databases from satellite data (*recognition criterion*); (ii) those showing the best consistency between sites (*universality criterion*); and (iii) those performing best at single sites (*local performance criterion*). The models are listed in Table 1 and categorized as a function of the number of their inputs, for reasons that will be discussed in Section 4.3. Model acronyms appear in small caps to distinguish them from their authors' names.

Some of the models examined here suffer from typographical errors in their published coefficient values, which makes their predictions inconsistent or sometimes even unphysical. This is the case for BOLAND2, POSADILLO, RUIZARIAS2, and TORRES1. The correct coefficients were directly obtained from their respective authors.

Tab. 1: General information on the 36 tested models. The predictors are: K_n , clearness index; K_{tcs} , clear-sky clearness index; K_{tm} , mean daily K_t ; t , local time; Z , zenith angle; m , air mass, ρ , surface albedo; V , variability index; RH , relative humidity, T , air temperature; T_{dpt} , dew-point temperature; E_{cs} , clear-sky global irradiance; E_{bncs} , clear-sky direct normal irradiance.

# Predictors	Model acronym	Author, Year	Predictor(s)	Remark on Model
1	BOLAND1	(Boland et al., 2008)	K_t	
	DEMIGUEL	(De Miguel et al., 2001)	K_t	
	ERBS	(Erbs et al., 1982)	K_t	
	HOLLANDS1	(Hollands, 1985)	K_t	
	LAM	(Lam and Li 1996)	K_t	Whole year model (Table 2)
	LI	(Li and Lam, 2001)	K_t	Whole year model (Table 1)
	LOUCHE	(Louche et al., 1991)	K_t	
	MONDOL	(Mondol et al., 2005)	K_t	
	MORENO	(Moreno et al., 2009)	K_t	
	MUNEER	(Muneer et al., 1997)	K_t	
	OLIVEIRA	(Oliveira et al., 2002)	K_t	
	REINDL1	(Reindl et al., 1990)	K_t	
	RUIZARIAS1	(Ruiz-Arias et al., 2010)	K_t	Model "G0"
	SANCHEZ	(Sanchez et al., 2012)	K_t	
	TORRES1	(Torres et al., 2010)	K_t	Model 1; corrected coefficient a8 in Table 1
TORRES2	(Torres et al., 2010)	K_t	"Model 3"	
2	GONZALEZ	(González and Calbó, 1999)	K_t, Z	
	HELBIG	(Helbig et al., 2010)	K_t, Z	
	HOLLANDS2	(Hollands and Crha, 1987)	K_t, ρ	
	MACAGNAN	(Macagnan et al., 1994)	K_t, Z	
	MAXWELL	(Maxwell, 1987)	K_t, m	
	POSADILLO	(Posadillo and Lopez Luque, 2009)	K_t, Z	Corrected coefficient in Eq. 10
	REINDL2	(Reindl et al., 1990)	K_t, Z	
	RIDLEY1	(Ridley et al., 2004)	K_t, t	
	RUIZARIAS2	(Ruiz-Arias et al., 2010)	K_t, m	Model "G2"; corrected coefficient in Eq. 19

	SKARTVEIT1	(Skartveit and Olseth, 1987)	K_t, Z	
	STAUTER	(Stauter and Klein, 1980)	K_t, K_{tc}	Paired with Hottel's clear-sky model
	SUEHRKE	(Suehrcke and McCormick, 1988)	K_t, m	
	ZHANG	(Zhang et al., 2004)	K_t, Z	
3	SKARTVEIT2	(Skartveit et al., 1998)	K_t, ρ, V	
4	PEREZ1	(Perez et al., 1992)	K_t, Z, T_{dp}, V	
	REINDL3	(Reindl et al., 1990)	K_t, Z, T, RH	
5	BOLAND2	(Boland et al., 2013)	K_t, Z, t, K_{tm}, V	Corrected coefficients in Eq. 4
	LAURET	(Lauret et al., 2013)	K_t, Z, t, K_{tm}, V	
	RIDLEY2	(Ridley et al., 2010)	K_t, Z, t, K_{tm}, V	
6	PEREZ2	(Perez et al., 2002)	$K_t, Z, T_{dp}, V, E_c, E_{bnc}$	Paired with Perez-Ineichen clear-sky model

3. Experimental data

Because separation models are empirical in nature, the robustness of their derivation directly depends on the quality of the data on which they are based. Data quality depends on many factors, including radiometer calibration, station maintenance, instrument cleaning, as well as radiometer specifications and performance. To decrease the impact of such factors on this analysis, only data from research-class stations are used here. A database of high-quality 1-min irradiance measurements has been assembled from nine stations located in arid or desert areas over five continents (Table 2). They all use thermopile radiometers and all independently measure the three components (direct, diffuse and global), which is necessary for thorough quality control postprocessing (Long and Shi, 2008; Roesch et al., 2011). Only data points passing these tests and for a zenith angle, Z , less than 85° are used here.

Some of the models tested here use more inputs than just K_t . A few use Z or air mass, m , which is not an issue because these are deterministic quantities. REINDL3 additionally requires temperature, T , and relative humidity, RH . Such variables are not always measured alongside irradiance or at the same frequency, which can cause problems, and ultimately can limit the applicability of the model. In the present case, T and RH are available at all sites except Alice Springs and Tamanrasset, where REINDL3 could thus not be tested. At Sede Boker, T and RH are only available in 10-min increments. They have been interpolated to 1-min steps with a cubic spline. PEREZ1 and PEREZ2 use dew-point temperature, T_{dp} , which is not measured at any of the sites under scrutiny here. Fortunately, T_{dp} can be derived from T and RH with appropriate empirical equations (typically used by meteorological services) for that purpose. The Perez models still work—albeit presumably in less optimum conditions—whenever T_{dp} is not available (Perez et al., 1992). This makes it possible to test them at all sites, including the two sites with no T, RH data.

HOLLANDS2 and SKARTVEIT2 require the surface albedo, ρ , which is rarely measured. A fixed default value was thus determined for each site, based on an educated guess. Two models, PEREZ2 and STAUTER, require an evaluation of clear-sky global and direct irradiance. For PEREZ2, the Perez-Ineichen model is used, as suggested and described by Perez et al. (2002), along with the popular monthly-mean, high-resolution Linke turbidity data described by Remund et al. (2003), and available from the SoDa service¹. For STAUTER, the Hottel model was used, as suggested in the original publication (Stauter and Klein, 1980). These clear-sky models have limited performance (Gueymard, 2012a; Gueymard and Ruiz-Arias, 2015), so slightly better DNI results could potentially be obtained with other radiation models.

Some separation models use information on the temporal variability of GHI through the use of a specific variability index, noted V in Table 1, which was originally developed from sequences of hourly irradiances immediately before and after the moment being modeled. The same algorithms are used here, therefore using 1-min sequences instead. Note that this definition of variability, as currently implemented in these models, can make them unfit for nowcasting or forecasting applications without proper adaptation. Similarly, a few models also use the daily-mean K_t as a predictor. This is not an issue here, but this requirement would also make them unfit for the aforementioned applications.

Tab. 2: General information on the nine test stations. N is the number of valid data points. The mean measured DNI is expressed in W/m^2 .

¹ http://www.soda-is.com/eng/services/climat_free_eng.php#c5

Station	Country	Data Source	Latitude (°)	Longitude (°)	Elevation (m)	Period	N	Mean DNI
Alice Springs	Australia	BSRN	19.539	-155.578	547	2009–2012	732457	667.2
Desert Rock, NV	USA	NOAA	36.626	-116.018	1007	2009–2013	971591	755.3
Gobabeb	Namibia	BSRN	-23.561	15.042	407	2012–2014	511578	741.5
Masdar	UAE	Masdar Inst.	24.442	54.617	6	2013	90530	544.0
PSA	Spain	DLR	37.091	-2.358	500	2011–2012	240047	571.1
Sede Boker	Israel	BSRN	30.860	34.779	480	2008–2011	719935	625.9
Solar Village	Saudi Arabia	BSRN	24.907	46.397	768	1999–2002	750872	585.6
Tamanrasset	Algeria	BSRN	22.790	5.529	1385	2006–2009	878736	621.7
Tucson, AZ	USA	NREL	32.230	-110.955	786	2011–2014	781236	685.5

4. Results and discussion

4.1 Statistical results

As discussed by Gueymard (2014), various statistical indicators can be used to evaluate the performance of DNI predictions. However, only conventional indicators are used here for conciseness: Mean Bias Deviation (MBD), Root Mean Square Deviation (RMSD), and Mean Absolute Deviation (MAD), all expressed in percent of the mean measured DNI at each station. These statistics are compiled in Table 3 for each model, considering all stations combined. This complete dataset contains $N = 5.677$ million data points, for an overall mean DNI of 662.4 W/m^2 . All statistics are expressed in percent of the latter value. It is difficult to compare the present results to those of the literature, because the latter most generally refer to DIF rather than DNI. A notable exception is the study of Perez et al. (1992), which reports hourly absolute errors relative to DNI (in W/m^2) for some of the same models used here, i.e., ERBS, MAXWELL and PEREZ1. The 1-min absolute RMSD found here for these three models averages to 112, 103 and 97 W/m^2 , respectively. These values are somewhat larger than the hourly RMS errors obtained by Perez et al. (1992) for the same models and the sunny/arid sites of Albuquerque and Phoenix, for instance. This suggests, as could be expected, that random errors increase with temporal resolution.

A graphical representation of these results, this time considering each test station separately, appears in Figs. 1–3. The best performer in each of the 6 model categories described in Table 1 is indicated by a color dot. For each station, the acronym of the best overall performer is also indicated. Note the significant scatter in the results at all sites. At Masdar, SUEHRKE appears as an outlier, with largest MBD, RMSD and MAD of all models and all sites. From Figs. 2 and 3, a remarkable localization effect clearly appears: RMSD and MAD are about twice as large at Tamanrasset than at Gobabeb, most likely because the former site has a much higher turbidity, which has a substantial effect on DNI (Gueymard, 2012b; Gueymard and Ruiz-Arias, 2015).

Table 3. Summary performance statistics (in percent of the overall mean DNI, 662.4 W/m^2) for all 36 tested models at all test sites combined. Best results in each category are in bold; best results overall are in bold italic and underlined.

Acronym	#Predictors	MBD	RMSD	MAD	Acronym	#Predictors	MBD	RMSD	MAD
BOLAND1	1	0.6	18.0	12.5	GONZALEZ	2	0.2	16.0	11.9
DEMIGUEL	1	-2.0	17.0	13.1	HELBIG	2	<u>0.0</u>	16.0	11.6
ERBS	1	-0.6	16.9	12.5	HOLLANDS2	2	-3.6	21.4	15.3
HOLLANDS1	1	2.0	18.7	12.6	MACAGNAN	2	1.2	18.6	14.1
LAM	1	-8.3	21.2	18.3	MAXWELL	2	4.3	15.6	10.6
LI	1	-4.9	18.6	15.4	POSADILLO	2	5.7	17.8	12.4
LOUCHE	1	5.0	17.4	11.4	REINDL2	2	-4.9	17.7	14.0
MONDOL	1	-7.7	18.8	16.0	RIDLEY1	2	-0.4	18.8	12.8
MORENO	1	6.7	19.3	13.0	RUIZARIAS2	2	-1.9	18.1	14.0
MUNEER	1	-4.7	17.9	14.1	SKARTVEIT1	2	-4.5	16.3	13.2
OLIVEIRA	1	0.2	17.2	13.0	STAUTER	2	-5.8	19.0	15.3
REINDL1	1	-0.4	16.9	12.5	SUEHRKE	2	-2.7	15.7	11.2
RUIZARIAS1	1	4.7	18.3	12.2	ZHANG	2	3.5	17.4	11.3
SANCHEZ	1	6.1	18.0	12.4	SKARTVEIT2	3	-3.9	16.5	12.6
TORRES1	1	-1.5	17.3	13.7	PEREZ1	4	5.3	14.7	9.7
TORRES2	1	-0.2	17.1	13.1	REINDL3	4	-0.4	12.5	9.5
					BOLAND2	5	1.4	15.8	11.0
					LAURET	5	4.3	17.4	11.3
					RIDLEY2	5	4.9	16.5	10.5

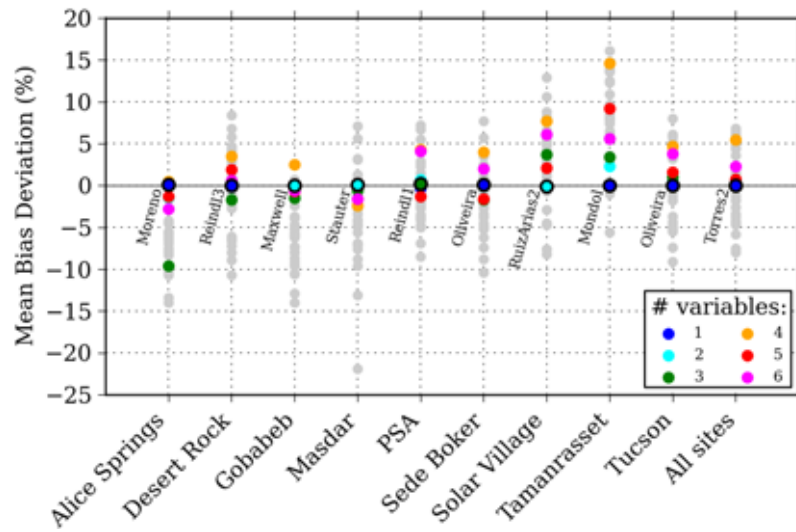


Fig. 1: MBD results for each station. In each category, the name of the best model is indicated, along with a color code.

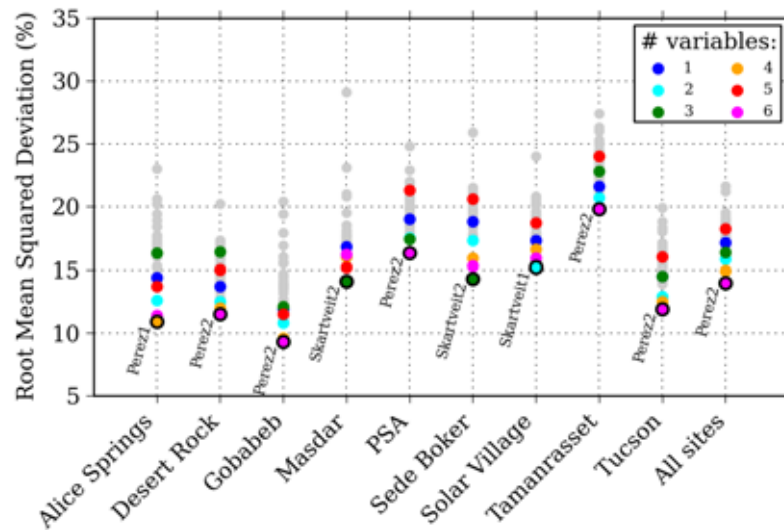


Fig. 2: Same as Fig. 1, but for RMSD.

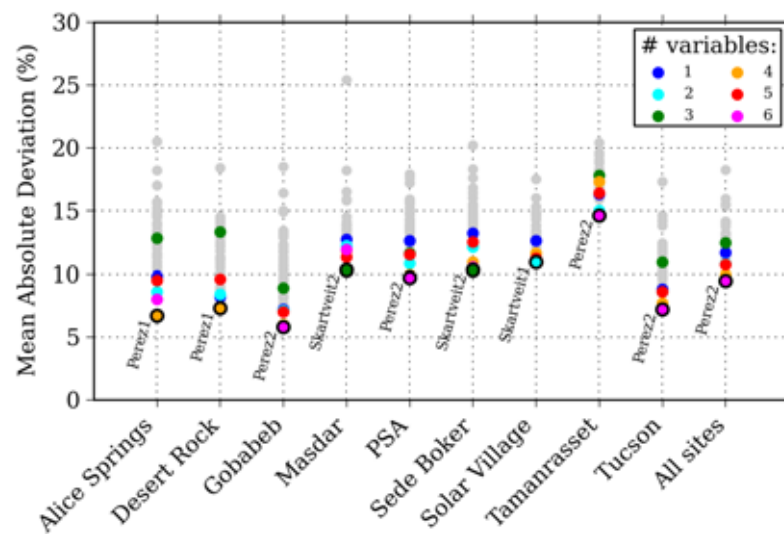
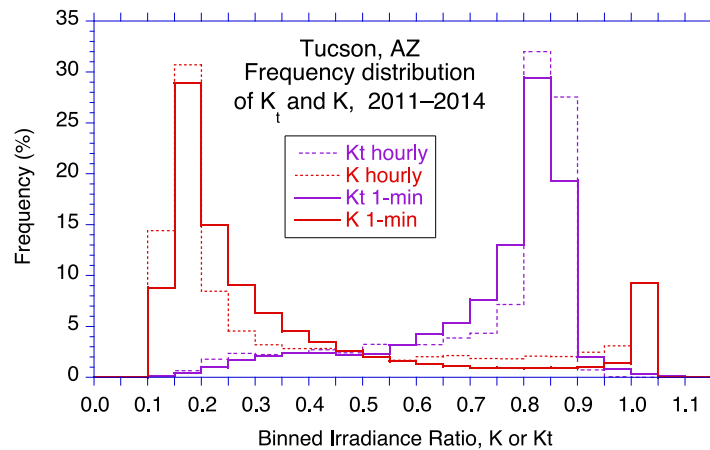


Fig. 3: Same as Fig. 1, but for MAD.

The results presented here tend to confirm previous studies, (e.g., Ineichen, 2008), to the effect that the Perez models (PEREZ1 and, even more so, PEREZ2) perform consistently better. The use of a 1-min variability index, rather than the hourly variability they were designed for, is therefore not detrimental to these two models. Arguably, their use of a variety of predictors in addition to K_t makes them more robust to changes in local conditions. However, this would also have benefitted other models with many predictors, such as REINDL3, BOLAND2, LAURET or RIDLEY2, which do not perform as consistently. The functional form of the Perez models thus appears as a key to their success. Surprisingly, however, the two Perez models usually have a non-negligible high bias (MBD). Conversely, those models with negligible bias do not perform as well as the Perez models with regard to the RMSD or MAD indicators. More discussion on these findings is offered in Section 4.3.

4.2 Impact of cloud enhancement and high irradiances

For CSP/CPV applications, what matters most is when DNI is high and around the design irradiance value. It is thus desirable to evaluate the performance of separation models when GHI and K_t are high too. Figure 4 shows the frequency distribution of K_t and K at Tucson, considering both hourly and 1-min data. Remarkably, significant differences in the K_t frequency distribution occur if $K_t > 0.65$. In particular, when $K_t > 0.9$, its hourly frequency is negligible, whereas its 1-min frequency is not. At the sites under scrutiny here, the absolute maximum value of 1-min K_t is typically ≈ 1.2 , which means that GHI can be occasionally 20% larger than its extraterrestrial counterpart—and still be a valid observation. This is caused by the cloud enhancement effect (also referred to as cloud lensing or over-irradiance), which is frequent under scattered cumulus cloud conditions when the sun is high. However, its magnitude decreases rapidly when time integration increases, which explains why such cases are much less noticeable in hourly data.

Fig. 4: Frequency distributions of hourly and 1-min K_t and K at Tucson.

Figures 5–7 show scatterplots of predicted vs. measured DNI for ERBS, LOUCHE and PEREZ2 at Tucson. The Erbs model (Fig. 5) is one of the most popular in the literature. Two issues are evident here: The S shape of its scatterplot, and the large fraction of overestimations when the measured DNI is larger than $\approx 400 \text{ W/m}^2$. This overestimation culminates when the measured DNI is $\approx 950 \text{ W/m}^2$ but predictions are (unphysically) up to $\approx 1400 \text{ W/m}^2$. This behavior can be explained by the functional form of the model: It assumes that K remains fixed at 0.165 when $K_t > 0.80$. By completely ignoring the cloud enhancement effect, the predicted K is much too low when $K_t > 0.9$, thus resulting in a largely overestimated DNI.

In Fig. 6, a similar S-shaped scatterplot is obtained for LOUCHE, another popular model. The behavior under high irradiance is different than with ERBS, however. A strong horizontal cluster is obvious for a predicted DNI of $\approx 1000 \text{ W/m}^2$, and a sizeable number of considerably underestimated outliers is found when the measured DNI is in the 800–1000 W/m^2 range—a pattern that does not exist in Fig. 5. This can be explained by the functional form of LOUCHE. It consists of a 5th-order polynomial providing $K_n = f(K_t)$, which reaches a maximum for $K_t = 0.86$ and then decreases, to the point where it becomes negative for $K_t > 1.05$. This produces unphysical values of the predicted DNI, which need to be zeroed out. Although such cases would not likely occur with hourly data, they do occur at 1-min resolution, then generating incorrect estimates.

The S shape of the ERBS and LOUCHE scatterplots is a feature that has apparently not been documented until

now. In any case, the issues described above explain why these two models do not perform as well as they could when using 1-min data, even though they may perform well with hourly data. In turn, this underlines the fact that not all hourly separation models work well with shorter time steps. Nevertheless, LOUCHE remarkably obtains the best overall MAD in its category of single-predictor models, and overall performs almost identically to LAURET, which uses 5 predictors (Table 3).

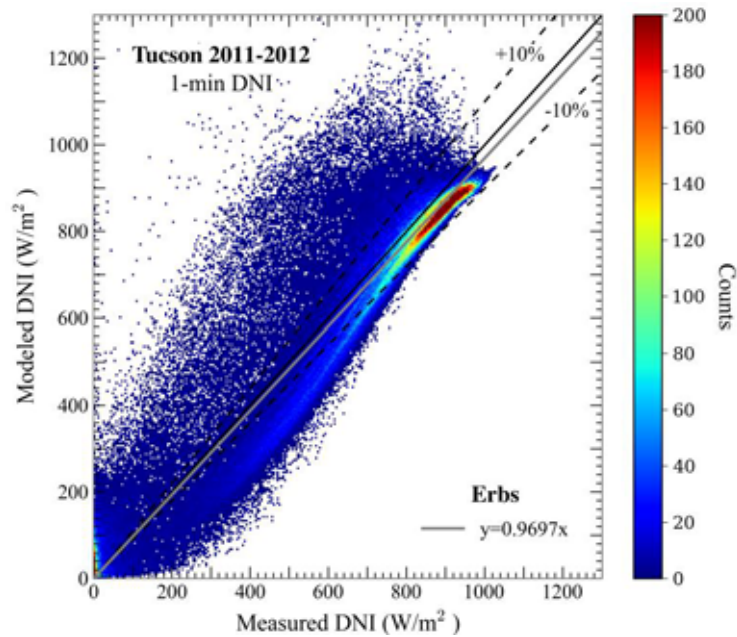


Fig. 5: Scatterplot of predicted vs. measured 1-min DNI using the ERBS model at Tucson

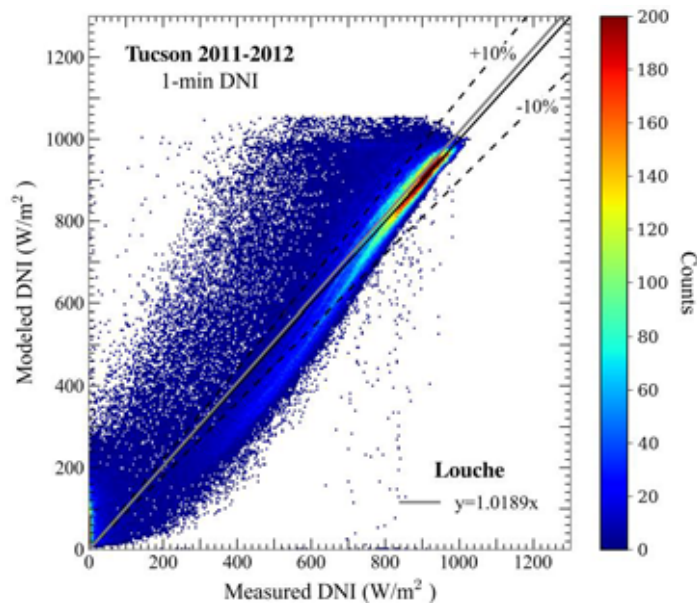


Fig. 6. Same as Fig. 5, but for the LOUCHE model

In contrast, Fig. 7 shows a similar scatterplot, but for PEREZ2, which obtains the best performance at Tucson (among other sites) with respect to the RMSD and MAD statistics. Its S shape is much less pronounced, and its predicted DNI is well clustered around the diagonal, at least above 700 W/m^2 . Still, there is a lot of scatter above the diagonal, and some outliers below it in the range $800\text{--}1000 \text{ W/m}^2$. This latter feature is similar, but much less pronounced, than with LOUCHE. The former issue can explain in large part why PEREZ2 (or PEREZ1 for that matter) tends to overestimate and surprisingly never performs best or too well with respect to MBD.

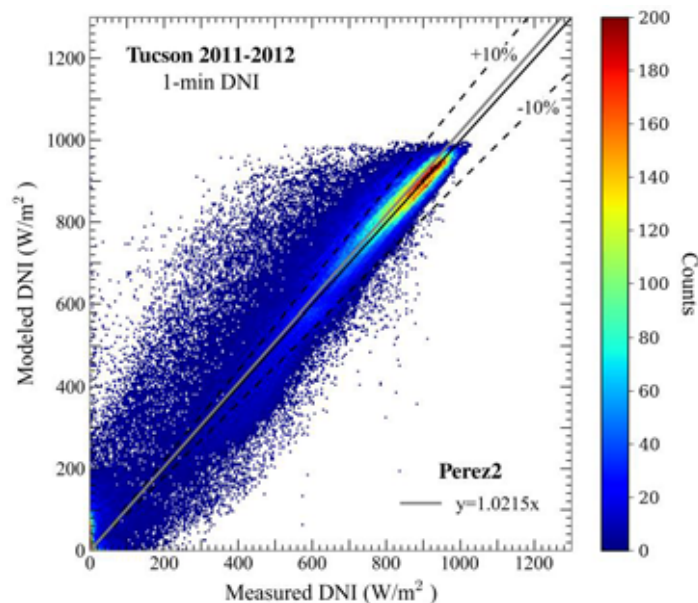


Fig. 7: Same as Fig. 5, but for the PEREZ2 model

4.3 Impact of the number of predictors

The present results clearly indicate that models based on many predictors, particularly if they include *variability*, tend to obtain the best results, as far as the RMSD and MAD performance indicators are concerned. A predictor is defined here as a single physical quantity, irrespective of how many times it appears in a functional form with different exponents, like in fifth-order polynomials for instance. In contrast, the total number of variables, including their different powers, is referred to here as “degree of freedom”. Thus, in the case a fifth-order polynomial of K_t is used, such as with LOUCHE, there are 5 degrees of freedom but just 1 predictor.

The variability-savvy models with the best results are PEREZ2, PEREZ1, SKARTVEIT2 and RIDLEY2, in decreasing frequency of appearance in the best rankings. Surprisingly, however, the two other models that include variability, LAURET and BOLAND2, do not perform as well. Equally surprising is that none of the variability-savvy models obtain the best rankings in terms of MBD. In any case, adding more predictors, most importantly variability, appears a potentially effective way to decrease random errors in separation models. This is logical, because these errors most frequently occur under partly cloudy conditions, which correspond to high variability in GHI. However, just adding variability as a predictor is not a guarantee in itself, since this predictor can interfere with other aspects of the model and eventually become counterproductive, as could be the case with LAURET and BOLAND2.

Some of the models reviewed here appear in different categories of Table 1, depending on the number of predictors of the various model variants proposed by their authors. This is the case for the REINDL (3 variants) and RUIZARIAS (2 variants) models. When developing a separation model, a central question is *which*, and thus *how many*, predictors should be used. A general trend in the literature has been to increase the number of predictors (and, sometimes, degrees of freedom too) in an attempt to also increase accuracy. Since all parameterizations are done empirically, a serious risk behind this approach is what is referred to as *overfitting*. Increasing the model’s degrees of freedom, or even the number of predictors, might indeed improve predictions for the sites where the parameterization was developed, but might as well degrade its *generalization* skill. Another aspect of this question is that some predictors might not be readily available locally, particularly at 1-min resolution, as already mentioned in Section 3.

When considering all results separately for each test station, the present results show that PEREZ1 performs better than PEREZ2 in one third of cases, which is contrary to expectations, since PEREZ2 has more predictors and was designed to improve on PEREZ1. This might be caused, at least in part, by inaccuracies in the clear-sky radiation model implied in PEREZ2 and/or its input data for specific sites. It is worth mentioning that using a clear-sky radiation model to directly obtain DNI from atmospheric data under cloudless situations is significantly more accurate than separating it from GHI (Gueymard, 2005). Similarly, the overall results in

Table 3 do not provide a clear answer about which variant of those models that offer multiple choices, such as REINDL and RUIZARIAS, has the potential to perform better under specific arid conditions. Typically, one variant performs better at some, but not all, sites, and results also differ depending on the performance indicator being used. For the 9 stations under scrutiny here, more detailed results are assembled in Table 4, in the form of the total number of stations where each model variant performs best relatively to a specific statistical indicator. The mixed results obtained in this example confirm the issue of performance rankings being dependent on the selected statistical indicator (Gueymard and Myers, 2008). A possible solution would consist in adopting a more robust indicator, such as the Combined Performance Index (Gueymard, 2012a, 2014). A detailed statistical analysis (using, e.g., the Bayesian Information Criterion) would also be desirable to evaluate whether adding predictors to a basic, simple model can improve its performance in a really *significant* way.

Tab. 4: Number of stations (out of a total of 9 for all models—except REINDL3, tested at 7 stations only) at which each model variant performs best according to different statistics.

Model	Best MBD	Best RMSD	Best MAD
REINDL1	4	4	4
REINDL2	2	3 (tied)	1
REINDL3	3	3 (tied)	4
RUIZARIAS1	4	4	7
RUIZARIAS2	5	5	2

5. Conclusion

A comprehensive statistical analysis of 36 separation models of the literature is described here. Their performance assessment is obtained by comparison of their DNI predictions with high-quality 1-min measured data obtained at 9 stations in different arid areas of the world where the DNI resource is high and thus favorable to the development of concentrating solar technologies, in particular. The uncertainty in the predicted DNI is found dependent on the specific separation model used, local specificities (such as atmospheric turbidity), as well as the number of predictors each model uses. The analysis thus considers a categorization of all models as a function of their number of predictors.

Some of those separation models that include a variability index tend to be more accurate than those that do not, but it is not a general conclusion, all the more that these models have usually more bias than simpler models and may generate spurious predictions. Models that use the clearness index as their single predictor do not necessarily perform worse than those using a higher number of predictors, except (in some but not all cases) if these include some description of variability.

Modeling issues are found in two models, which prevent them to perform as efficiently with 1-min data than with the hourly data for which they were designed. This finding is directly related to the significant impact of cloud enhancement on 1-min data, which may temporarily increase the clearness index to over-unity values.

It is hoped that the present findings will help stimulate the development of advanced functional forms for this type of radiation model. Indeed, to improve the accuracy of DNI predictions at high frequency and decrease their current noise, an obvious conclusion is that a more efficient and truly “universal” model is necessary. Since the statistical results presented here—as well as the ranking of models that can be derived from them—are dependent on local conditions and statistical indicator, more validation studies are desirable to evaluate which model performs best over any specific region, with the help of more advanced statistical tools.

6. Acknowledgments

The authors express their gratitude to the dedicated personnel who maintain the radiometric stations whose high-quality measurements have been central to this study. The PSA and Masdar data were kindly provided by Stefan Wilbert and Peter Armstrong, respectively, whose collaboration is highly appreciated.

7. References

- Boland, J., Huang, J., Ridley, B., 2013. Decomposing global solar radiation into its direct and diffuse components. *Renew. Sust. Energy Rev.* 28, 749-756.
- Boland, J., Ridley, B., Brown, B., 2008. Models of diffuse solar radiation. *Renew. Energy* 33, 575-584.
- De Miguel, A., Bilbao, J., Aguiar, R., Kambezidis, H.D., Negro, E., 2001. Diffuse solar irradiation model evaluation in the north Mediterranean belt area. *Solar Energy* 70, 143-153.
- Erbs, D., Klein, S.A., Duffie, J.A., 1982. Estimation of the diffuse radiation fraction for hourly, daily and monthly average global radiation. *Solar Energy* 28, 293-302.
- González, J.A., Calbó, J., 1999. Influence of the global radiation variability on the hourly diffuse fraction correlations. *Solar Energy* 65, 119-131.
- Gueymard, C.A., 2005. Importance of atmospheric turbidity and associated uncertainties in solar radiation and luminous efficacy modelling. *Energy* 30, 1603-1621.
- Gueymard, C.A., 2009. Direct and indirect uncertainties in the prediction of tilted irradiance for solar engineering applications. *Solar Energy* 83, 432-444.
- Gueymard, C.A., 2012a. Clear-sky irradiance predictions for solar resource mapping and large-scale applications: Improved validation methodology and detailed performance analysis of 18 broadband radiative models. *Solar Energy* 86, 2145-2169.
- Gueymard, C.A., 2012b. Temporal variability in direct and global irradiance at various time scales as affected by aerosols. *Solar Energy* 86, 3544-3553.
- Gueymard, C.A., 2014. A review of validation methodologies and statistical performance indicators for modeled solar radiation data: Towards a better bankability of solar projects. *Renew. Sustain. Energy Rev.* 39, 1024-1034.
- Gueymard, C.A., Myers, D.R., 2008. Validation and ranking methodologies for solar radiation models, in: Badescu, V. (Ed.) *Modeling Solar Radiation at the Earth Surface*, Springer.
- Gueymard, C.A., Ruiz-Arias, J.A., 2015. Validation of direct normal irradiance predictions under arid conditions: A review of radiative models and their turbidity-dependent performance. *Renew. Sust. Energy Rev.*, in press.
- Helbig, N., Löwe, H., Mayer, B., Lehning, M., 2010. Explicit validation of a surface shortwave radiation balance model over snow-covered complex terrain. *J. Geophys. Res.* 115D, doi:10.1029/2010JD013970.
- Hirsch, T., Schenk, H., Schmidt, N., Meyer, R., 2010. Dynamics of oil-based parabolic trough plants—Impact of transient behaviour on energy yields. *Proc. SolarPACES Conf.*, Perpignan, France.
- Hollands, K.G.T., 1985. A derivation of the diffuse fraction's dependence on the clearness index. *Solar Energy* 35, 131-136.
- Hollands, K.G.T., Crha, S.J., 1987. An improved model for diffuse radiation: Correction for atmospheric back-scattering. *Solar Energy* 38, 233-236.
- Ineichen, P., 2008. Comparison and validation of three global-to-beam irradiance models against ground measurements. *Solar Energy* 82, 501-512.
- Lam, J.C., Li, D.H.W., 1996. Correlation between global solar radiation and its direct and diffuse components. *Build. Environ.* 31, 527-535.
- Lauret, P., Boland, J., Ridley, B., 2013. Bayesian statistical analysis applied to solar radiation modelling. *Renew. Energy* 49, 124-127.
- Li, D.H.W., Lam, J.C., 2001. Analysis of solar heat gain factors using sky clearness index and energy implications. *Energy Convers. Manag.* 42, 555-571.
- Long, C.N., Shi, Y., 2008. An automated quality assessment and control algorithm for surface radiation measurements. *Open Atmos. Sci. J.* 2, 23-37,

- Louche, A., Notton, G., Poggi, P., Simonnot, G., 1991. Correlations for direct normal and global horizontal irradiation on a French Mediterranean site. *Solar Energy* 46, 261-266.
- Macagnan, M., Lorenzo, E., Jimenez, C., 1994. Solar radiation in Madrid. *Int. J. Solar Energy* 16, 1-14.
- Maxwell, E.L., 1987. A quasi-physical model for converting hourly global horizontal to direct normal insolation. *Proc. Solar '87, Annual ASES Conf., Portland, OR, American Solar Energy Soc.*
- Mondol, J.D., Yohanis, Y.G., Smyth, M., Norton, B., 2005. Long-term validated simulation of a building integrated photovoltaic system. *Solar Energy* 78, 163-176.
- Moreno, S., Silva, M., Fernandez-Peruchena, C.M., Pagola, I., 2009. Comparison of methodologies to estimate direct normal irradiation from daily values of global horizontal irradiation. *Proc. SolarPACES Conf., Berlin, Germany.*
- Muneer, T., Kambezidis, H., Tregenza, P., 1997. *Solar radiation and daylight models for the energy efficient design of buildings.* Architectural Press.
- Oliveira, A.P., Escobedo, J.F., Machado, A.J., Soares, J., 2002. Correlation models of diffuse solar-radiation applied to the city of Sao Paulo, Brazil. *Appl. Energy* 71, 59-73.
- Perez, P., Ineichen, P., Moore, K., Kmiecik, M., Chain, C., George, R., Vignola, F., 2002. A new operational model for satellite-derived irradiances: Description and validation. *Solar Energy* 73, 307-317.
- Perez, R., Ineichen, P., Maxwell, E.L., Seals, R., Zelenka, A., 1992. Dynamic global-to-direct irradiance conversion models. *ASHRAE Trans.* 98 (1), 354-369.
- Posadillo, R., Lopez Luque, R., 2009. Hourly distributions of the diffuse fraction of global solar irradiation in Córdoba (Spain). *Energy Convers. Manag.* 50, 223-231.
- Reindl, D.T., Beckman, W.A., Duffie, J.A., 1990. Diffuse fraction correlations. *Solar Energy* 45, 1-7.
- Remund, J., Wald, L., Lefèvre, M., Ranchin, T., Page, J., 2003. Worldwide Linke turbidity information. *Proc. ISES Conf., Stockholm, Sweden, International Solar Energy Society.*
- Ridley, B., Boland, J., Lauret, P., 2010. Modelling of diffuse solar fraction with multiple predictors. *Renew. Energy* 35, 478-483.
- Ridley, B., Boland, J., Luther, M., 2004. Quality control of climate data sets *Proc. Solar 2004: Life, the Universe and Renewables, Murdoch University, Australia, ANZSES.*
- Roesch, A., Wild, M., Ohmura, A., Dutton, E.G., Long, C.N., Zhang, T., 2011. Assessment of BSRN radiation records for the computation of monthly means. *Atmos. Meas. Tech.* 4, 339-354; Corrigendum, www.atmos-meas-tech.net/334/973/2011/.
- Ruiz-Arias, J.A., Alsamamra, H., Tovar-Pescador, J., Pozo-Vazquez, D., 2010. Proposal of a regressive model for the hourly diffuse solar radiation under all sky conditions. *Energy Convers. Manag.* 51, 881-893.
- Sanchez, G., Cancillo, M.L., Serrano, A., 2012. Adapting the Spencer model for diffuse solar radiation in Badajoz (Spain). *Opt. Pura Apl.* 45, 5-9.
- Skartveit, A., Olseth, J.A., 1987. A model for the diffuse fraction of hourly global radiation. *Solar Energy* 38, 271-274.
- Skartveit, A., Olseth, J.A., Tuft, M., 1998. An hourly diffuse fraction model with correction for variability and surface albedo. *Solar Energy* 63, 173-183.
- Stauter, R., Klein, S.A., 1980. Unpublished work, in: Duffie, J.A., Beckman, W. (Eds.) *Solar Engineering of Thermal Processes*, Wiley, New York.
- Suehrcke, H., McCormick, P.G., 1988. The diffuse fraction of instantaneous solar radiation. *Solar Energy* 40, 423-430.
- Torres, J.L., de Blas, M., Garcia, B., de Francisco, A., 2010. Comparative study of various models in estimating hourly diffuse solar irradiance. *Renew. Energy* 35, 1325-1332.

Zhang, Q.Y., Lou, C., Yang, H., 2004. A new method to separate horizontal solar radiation into direct and diffuse components. Proc. ISES Asia-Pacific Conf., Gwangju, Korea, International Solar Energy Society.